Prospects for Gamma-Ray Burst detection by the Cherenkov Telescope Array

E. Bissaldi[1][2][*], T. Di Girolamo[3][4], F. Di Pierro[5], T. Gasparetto[6], F. Longo[6][7], P. Vallania[5][8] and C. Vigorito[5][9]

for the CTA Consortium[10]

[1] *Politecnico di Bari –Bari, Italy*
[2] *INFN, Sezione di Bari – Bari, Italy*
[3] *Università di Napoli "Federico II" – Napoli, Italy*
[4] *INFN, Sezione di Napoli – Napoli, Italy*
[5] *INFN, Sezione di Torino – Torino, Italy*
[6] *Università degli Studi di Trieste – Trieste, Italy*
[7] *INFN, Sezione di Trieste-Udine – Trieste, Italy*
[8] *INAF, Osservatorio Astrofisico di Torino – Torino, Italy*
[9] *Università degli Studi di Torino – Torino, Italy*
[10] *See* `www.cta-observatory.org` *for full author & affiliation list*

Summary. — The Large Area Telescope (LAT) on the Fermi satellite is expected to publish a catalogue with more than 100 Gamma-Ray Bursts (GRBs) detected above 100 MeV thanks to a new detection algorithm and a new event reconstruction. This work aims at revising the prospects for GRB detection with the Cherenkov Telescope Array (CTA) based on the new LAT results. We start considering the simulation of the observations with the full CTA of 10 bright GRBs detected by Fermi-LAT. In the future we plan to investigate how these GRBs would be observed by different subsamples of the array pointing to different directions.

1. – The CTA observatory

The Cherenkov Telescope Array (CTA) is a worldwide project aiming at building and operating the next generation of Imaging Atmospheric Cherenkov Telescopes (IACTs). In its baseline design, two huge arrays are foreseen, one in the Southern (Paranal, Chile) and one in the Northern (La Palma, Spain) hemisphere. In its current design, more than 100 telescopes will extend the energy range of currently operating IACTs both at lower and higher energies and will improve the sensitivity by about one order of magnitude with

---

(*) Corresponding author – Email: elisabetta.bissaldi@ba.infn.it

better angular and energy resolutions. In order to achieve this goal, a combination of different types of telescopes is necessary. Large Size Telescopes (LSTs), with a diameter of 23 m and placed at a distance of 100 m from each other, will observe the energy region between ∼20 and ∼200 GeV in both the Northern and Southern sites. Near the energy threshold, the number of source photons is relatively high but the Cherenkov image is poor, therefore a few huge telescopes are used to collect faint showers. Medium Size Telescopes (MSTs), with a diameter of 12 m, will be sensitive in the energy range between ∼100 GeV and ∼10 TeV, arranged on an area of about 1 km^2 (Southern site) and 0.2 km^2 (Northern site). At these energies, the Cherenkov signal starts to increase while the source flux rapidly fades, so an intermediate choice for number and dimensions of the telescopes is optimal. Small Size Telescopes (SSTs), with a diameter of 4 m, will operate in the energy range between ∼5 and ∼300 TeV, and will cover a 3–4 km^2 area. The CTA baseline array layout consists of 4 LSTs, 25 MSTs and 70 SSTs in the Southern Site (where most of the Galactic plane is visible), and 4 LSTs and 15 MSTs in the Northern Site.

2. – High-energy GRB observations

Gamma-Ray Bursts (GRBs) represent a very interesting case study in astrophysics, mainly due to their multi-disciplinary nature. Presently, a GRB can trigger one or more of the dedicated instruments based on several satellites orbiting around the Earth, such as Swift, Fermi, MAXI or INTEGRAL. The observed keV–MeV prompt emission may be accompanied by an X–ray, optical or radio afterglow. Rapid follow–up of the prompt keV–MeV emission is possible thanks to communication through the Gamma–ray Coordinates Network (GCN), where the GRB position is spread out in real time to all other observatories. This includes all currently operative IACTs like MAGIC, H.E.S.S., and VERITAS. Unfortunately, none of them ever succeeded in capturing a high–energy signal from a GRB, but several upper limits from a single or from a sample of bursts were published by each collaboration over the last years.

Current prospects for very high–energy GRB observations by CTA [1, 2] are based on extrapolations taken either from the GRB spectral parameters published in the catalogs of the Burst and Transient Source Experiment (BATSE, 20 keV–2 MeV) and of the Swift Burst Alert Telescope (BAT, 15–150 keV), or from some very energetic GRBs detected by the Fermi instruments before 2012. Our aim is to expand these samples with the newest results obtained by both instruments on–board Fermi, namely the Gamma-Ray Burst Monitor (GBM, 8 keV–40 MeV) and the Large Area Telescope (LAT, ∼30 MeV–300 GeV). We are currently preparing a library of GRBs observed at different post-trigger epochs, which includes ∼1000 GRBs from the second GBM spectral catalog [3], 35 GRBs from the first LAT GRB catalog [4], and ∼130 new GRBs from the second LAT GRB catalog (in preparation, [5]). For a subset of these GRBs redshifts are also known.

3. – Simulation of GRB observations

To estimate the detectability of a burst, we make use of the `ctools`, a software package specifically developed for the scientific analysis of CTA data (v0.9.0)([1]). For each GRB, we assume that both the observed flux and the time decay of the integrated light follow
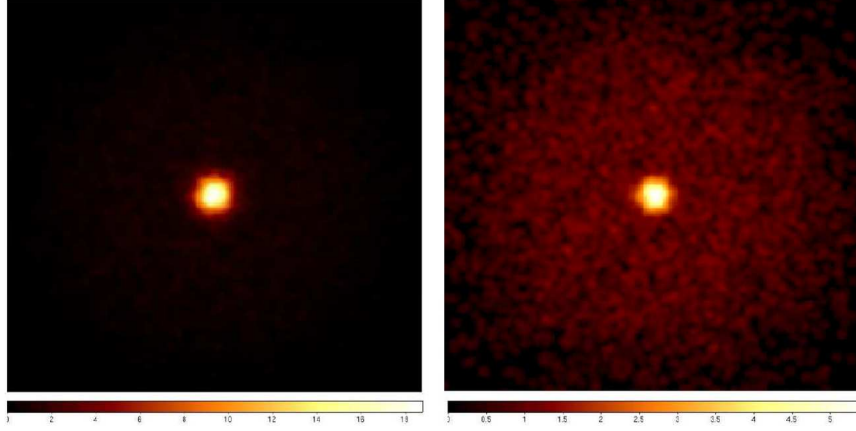

([1]) http://cta.irap.omp.eu/ctools/index.html

Fig. 1.: Simulations of GRB 130427A with `ctools`. The camera images are divided into 200×200 bins of 0.02°. The color scale gives the counts/bin after Gaussian smoothing. Left panel: Count map for an observation lasting 10 min starting from 1 ks after the trigger. Right panel: Count map for an observation lasting 0.5 hr starting from 10 ks after the trigger.

a power law decay, i.e. $(dN/dE) \propto E^{-\beta}$ and $(dN/dt) \propto t^{-\alpha}$ is assumed. Moreover, we assume that the bursts are observed on axis and at a zenith angle $\theta = 20°$, with the CTA North array. We also consider an optimistic repointing time t_r of 20 seconds for the LST of CTA. In all simulations, the index of the PL spectra does not vary with time. Our GRB sample comprises 10 bursts seen by the LAT. 9 are included in [4], and one is GRB 130427A, a very luminous GRB observed after the catalog was published and which represents the current record holder of the highest energy photon ever observed from a GRB (95 GeV).

The first test case is GRB 130427A. The average flux between 10 ks and 70 ks was measured by the LAT in the range 0.1–100 GeV, and had a value of $6.7 \pm 2.0 \cdot 10^{11}$ ph/cm^2/s/MeV at 826 MeV, with a spectral index of 2.2 ± 0.2 [6]. We performed an analysis with ctools in the energy range 100 GeV to 1 TeV adopting a spectral model obtained by extrapolating the LAT PL index to higher energies. We obtained an integral flux of $3 \cdot 10^{12}$ erg/cm^2/s, which is compatible to the upper limit obtained by VERITAS [10]. We then simulated two possible observations by CTA, namely (A) a small time-window at early post-trigger times, and (B) a large time-window at late post–trigger times. For GRB 130427A, we simulated observation (A) lasting 10 min at $t_r = 1$ ks post trigger and observation (B) lasting half an hour at $t_r = 10$ ks post trigger. We also included the effect of the EBL absorption, using the EBL model of [9]. Results are shown in two count maps in fig. 1. Count maps can be obtained using the `ctools` functions `ctobssim` and `ctbin` and adopting the official CTA instrument response functions (IRFs)[2]. We made use of the *North_0.5h* IRF for observation (A) and of the *North_5h* IRF for observation (B). The decision of using a more conservative IRF for longer observations was driven by the need of reducing the increased background contribution.

---

[2] https://www.cta-observatory.org/science/cta-performance/

TABLE I.: Parameters used to simulate the sample of 10 GRBs, namely the peak flux F_P, the spectral and temporal indexes β and α, and the peak–flux time t_P. Data for the first 9 GRBs are taken from table 4 of [4]. Data for GRB130427A are taken from [10].

Name	F_p (ph/cm^2/s $\times 10^{-5}$)	Spec.index [β]	Time index [α]	$t_p(s)$
GRB080916C	500±100	2.05±0.07	1.37 ± 0.07	6.6 ± 0.9
GRB090323	6±3	2.3±0.2	1.0 ± 0.3	40 ± 30
GRB090328	9±4	2.0±0.2	1.0 ± 0.3	40 ± 30
GRB090510	3900±600	2.05±0.07	1.8 ± 0.2	0.9 ± 0.1
GRB090902B	600±100	1.95±0.05	1.56 ± 0.06	9 ± 1
GRB090926A	700±100	2.12±0.07	1.9 ± 0.2	11 ± 2
GRB091003	8±3	2.1±0.2	1.0 ± 0.2	22 ± 9
GRB100414	70±30	2.0±0.2	1.7 ± 0.3	20 ± 10
GRB110731A	220±60	2.4±0.2	1.8 ± 0.2	4.8 ± 0.7
GRB130427A	150±30	2.2±0.2	1.35 ± 0.08	20 ± 5

We then moved on to and studied the other 9 GRBs. The spectral and temporal parameters used in the analysis are reported in tab. I. For these bursts, we extrapolated the flux from the LAT energy range to the CTA energy range. Knowing the peak flux F_P and the peak–flux time t_P, we can derive the flux at repoint time adopting the relation $F(t_r) = F_P(t_r/t_P)^{-\alpha}$. We also divided the observation period (two days) into 20 time bins (with logarithmic spacing) and calculated the flux as an average value during that interval. In order to study the effect of the EBL absorption, we modified the spectral slope of each GRB placing it at different redshifts, ranging from 0.1 to 3.0. Figure 2 shows the spectral slopes derived for GRB 080916C as it was placed, with the same observed flux, at different redshift. It can be seen that the low energy part of the model (up to an energy of 20 GeV) is redshift–independent, while increasing the redshift corresponds to a stronger absorption. Finally, we simulated the source in each bin, fitted it and determined the significance of the detection by means of the test statistics (TS) parameter. Results
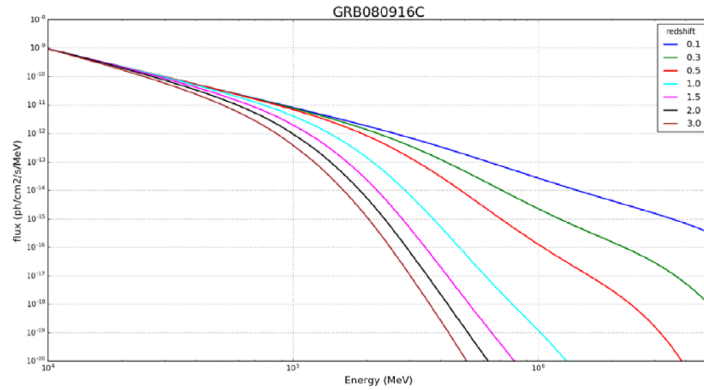

Fig. 2.: Study of EBL absorption for GRB 080916C placed at 7 different redshifts.
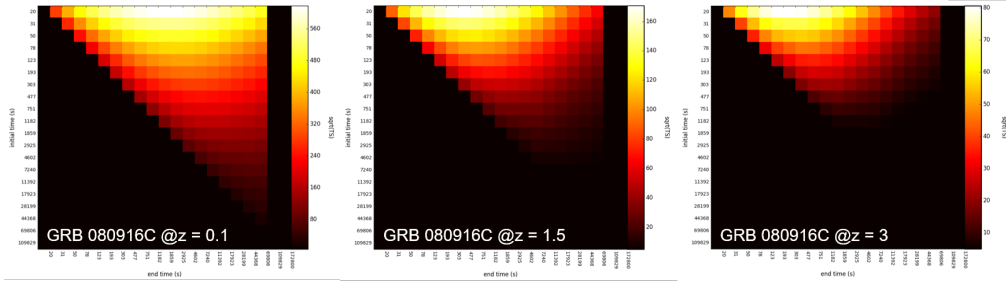
Fig. 3.: TS maps (z-axis) versus start (y-axis) and end time (x-axis) of the simulation for GRB 080916C placed at three different redshifts.

are displayed as 2D maps of TS values versus time, which we generated for every GRB and every redshift. An example is given in fig. 3, where we show evolution of the 2D map of GRB 080916C for three different values of the redshift (0.1, 1 and 3). An increasing redshift and shorter observation determine a drop in TS.

* * *

REFERENCES

[1] INOUE S. ET AL., *Astroparticle Physics*, **43** (2012) 252.
[2] GILMORE R. ET AL., *Experimental Astronomy*, **35** (2013) 413.
[3] GRUBER D. ET AL., *Astrophysical Journal, Supplement*, **211** (2014) 12.
[4] ACKERMANN M. ET AL., *Astrophysical Journal, Supplement*, **209** (2013) 11.
[5] VIANELLO G. ET AL., *American Astronomical Society Meeting*, **227** (2016) id.416.01.
[6] ACKERMANN M. ET AL., *Science*, **343** (2014) 42.
[7] ACKERMANN M. ET AL., *Astrophysical Journal*, **716** (2010) 1178.
[8] DE PASQUALE M. ET AL., *Astrophysical Journal, Letters*, **709** (2010) 146.
[9] FRANCESCHINI A. ET AL., *Astronomy & Astrophysics*, **487** (2008) 837.
[10] ALIU E. ET AL., *Astrophysical Journal*, **795** (2014) 1.